Lisha ZHU
Yimin ZHANG
Rui ZHANG
Peiming ZHANG

TIME-DEPENDENT RELIABILITY OF SPUR GEAR SYSTEM BASED ON GRADUALLY WEAR PROCESS

ZALEŻNA OD CZASU NIEZAWODNOŚĆ UKŁADU PRZEKŁADNI ZĘBATEJ JAKO FUNKCJA PROCESU STOPNIOWEGO ZUŻYCIA

To study dynamic evolution law of mechanical reliability caused by wear, gear transmission system is taken as a research object. Considering the effect of clearance caused by wear on gear teeth load in double meshing area, the formula of dynamic distribution load which is undertaken by two adjacent teeth is deduced. And the distributed pressure and meshing speed, which should be taken into account while calculating gear wear, are obtained based on the Winkler surface model and principle of tooth mesh. Based on the Archard's wear model, numerical simulation model for wear in spur gear is deduced, and the wear depth of each meshing points on teeth outline with different wear cycles are obtained. The calculation wear model is replaced with a surrogate model with Neural Network and Kriging method to overcome time-consuming defect. Random process model is integrated with the surrogate model, and dynamic reliability for nonlinear stochastic structure with unknown distribution characteristic is obtained with Neural Network-based Edgeworth series technique and four moment methods, which is compared with Kriging-based Monte Carlo simulation method. The computational efficiency and accuracy are also demonstrated.

Keywords: reliability; gear; time-dependent; wear; gradually.

W artykule badano prawo dynamicznej ewolucji niezawodności mechanicznej powodowanej zużyciem na przykładzie układu przekładni zębatej. Na podstawie rozważań nad wpływem luzu powstałego na skutek zużycia na obciążenie zębów przekładni w obszarze podwójnych zazębień, wyprowadzono wzór na dynamiczny rozkład obciążeń przyjmowanych przez pary sąsiadujących zębów. Rozłożone naciski i prędkość zazębiania, które należy uwzględnić przy obliczaniu zużycia przekładni, otrzymano na podstawie modelu powierzchniowego Winklera oraz zasady zazębienia. W oparciu o model zużycia Archarda, wyprowadzono numeryczny model symulacyjny zużycia w przekładni zębatej oraz obliczono głębokość zużycia każdego z punktów zazębienia na zarysie zębów przy różnych cyklach zużycia. Aby uniknąć problemu czasochłonności, obliczeniowy model zużycia zastąpiono modelami zastępczymi bazującymi na sieci neuronowej i metodzie krigingu. Model procesu losowego zintegrowano z modelem zastępczym, a dynamiczną niezawodność dla nieliniowej struktury stochastycznej o nieznanej charakterystyce rozkładu uzyskano za pomocą techniki serii Edgeworth opartej na sieci neuronowej oraz metody czterech momentów, którą porównano z metodą symulacji Monte Carlo opartą na krigingu. Wykazano także wydajność obliczeniową i dokładność omawianej metody.

Słowa kluczowe: niezawodność; koło zębate; zależność od czasu; zużycie; stopniowy.

1. Introduction

Friction and wear are unavoidable for transmitting power in gear systems. Severe wear can cause mechanical component damage. The dynamic characteristic of gear system is affected not only by friction and wear but also by variation of geometrical shape and dimension parameter caused by mild wear, which lead to more serious wear. Therefore, the coupled relation between wear and dynamic load should be taken into consideration to study gear wear.

Gear parameters might not be accurate after machining in practice, which is one of reasons why product failure still occurs. That is to say, parameters have uncertainty and randomness. Besides, wear depth accumulates over time gradually, so gear wear is a random process, which has random statistical regularity. As a result, more practical surface wear model and dynamic reliability model with gradually parameters can be established from the definition of reliability, the reliability of mechanical component can be observed all over its life cycle, and the tolerance of designed parameters can be determined to reduce failure probability.

The wear model should be established based on failure mechanism to study gear wear. In recent 30 years, wear and failure mechanism of gears have been studied based on lots of laboratory tests, Zurowski[28] et al. employed TT-3 tester to research wear resistance of C45（norm）/145Cr6 and C45(600)/145Cr6 matchings and indicated that wear resistance of the two matchings had a significant dependence on friction area temperature and material hardness. However, research on establishing models and calculation methods for gear wear have little been touched on. In general, these models break down into three categories:

The first model was established on undetermined coefficient or regression analysis method according to test data. The conclusion was convincing but only obtained laws for intermediate variables. For example, Põdra[15] studied wear had a linear correlation with normal load and had incomplete correlation with sliding velocity.

The second was developed to discuss the influence of parameters from energy loss aspect. For example, Onishchenko[14] studied the effect of machine operation, corresponding tribological theories, the eccentricity of pitch circle and the instant temperature in the contact

on wear. The model stated that wear is simply proportional to specific power, which needed further study.

The third was the Archard wear model[3] which had been widely adopted. The formula had evolved from severe sliding of intermeshing tooth. Andersson[2] obtained analytical formula of sliding distance which varied with different mesh position. Flodin and Andersson[9] developed a numerical model for wear prediction of spur gear and the contact were modelled by Winkler's elastic foundation model. Park[16] combined Archard's wear model with a finite-element based hypoid gear contact model for simulation of surface wear of hypoid gear pairs. Most of the above adopted equal or linear distributed load[2,4,6], without coupled relations between tooth load and wear. Flodin[8,9] studied the effect of spur gears on contact condition, whereas, the sequence of contact, clearance size between two adjacent teeth and time-varying stiffness were not considered.

The parameters were deterministic in the wear models above, randomness of excited load and gradual wear were also not considered. As a matter of fact, wear-based reliability of mechanical product is varying gradually with time[22]. There are many methods to build time-dependent reliability model, such as Markov theory[19], dynamic fault-tree model[7,13], stochastic MCS model[5], Go-flow model[11], stochastic petri nets[20]. As mechanical structure is so complex that the methods above are hardly applied to dynamic reliability analysis for mechanical systems and components. One is because the relationship between response and parameters are nonlinear and there is no analytic expression for the state limited function in general. The other is lack of statistical data and distribution law for parameters.

Reliability analysis is based on probability analysis and mathematical statistics, so it needs enough samples to determine probability characteristic of variables and response. Therefore, it would be time-consuming to obtain enough samples for complex structure. To establish reliability model for complex structure system, the accurate numerical model is replaced with one of surrogate models based on response surface, neutral network, radial basis function network, support vector machine and kriging method, and reliability are obtained by surrogate-model-based monte carlo simulation method. Gomes and Awruch[10] presented response surface and artificial neural network techniques to solve complex and more elaborated problems and carried out comparison using FORM, direct MCS and MCS with adaptive importance sampling. Tan[18] proposed radial basis function networks and support vector machines for reliability analysis. Zhu and Du[27] applied the kriging-based MCS method which was suitable for highly nonlinear limit-state functions to reduce the computational cost. Because the nonlinear response with complex structure can be rapidly predicted in any design point using a kriging interpolator and the iteration process has higher stabilization and faster convergence speed than other methods, the Kriging model is employed in the present paper.

To solve the problem of unknown distribution, on the basis of the surrogate model, Edgeworth series and Four moment techniques are suitable for reliability analysis. The method combines analysis method and moment method and Zhang[26] developed a statistical fourth moment method to examine reliability of the rotor-stator systems with rubbing. All the models and methods above have not been used in analysing wear-based reliability of gear system.

In the present paper, a numerical wear model for a pair of spur gears is established considering coupled relation of wear and dynamic load. A time-dependent reliability model with gradual parameters is also build under the condition that original parameters are stochastic and wear is gradually changing. The time-varying reliability curves for spur gears are obtained during the life cycle.

2. Load distribution theory

As shown in Figure 1, in one meshing cycle, single teeth-meshing area and double teeth-meshing area appear alternately. In single teeth-meshing area, the transmission load is carried only by one pair of mesh gear. In double teeth-meshing area, the transmission load is carried by two pairs of mesh gear. If only considering elastic deformation without wear, the two pairs of mesh gear can be regarded as parallel springs. The distribution load is calculated according to time-varying stiffness of every pair. However, clearance is formed among teeth pair caused by wear in gears, which are run in low speed and heavy load, thus meshing point will deviate from its normal involute location. So, it is necessary to consider time-varying meshing stiffness, the sizes of the two clearances and the contact sequence of the two teeth pairs.
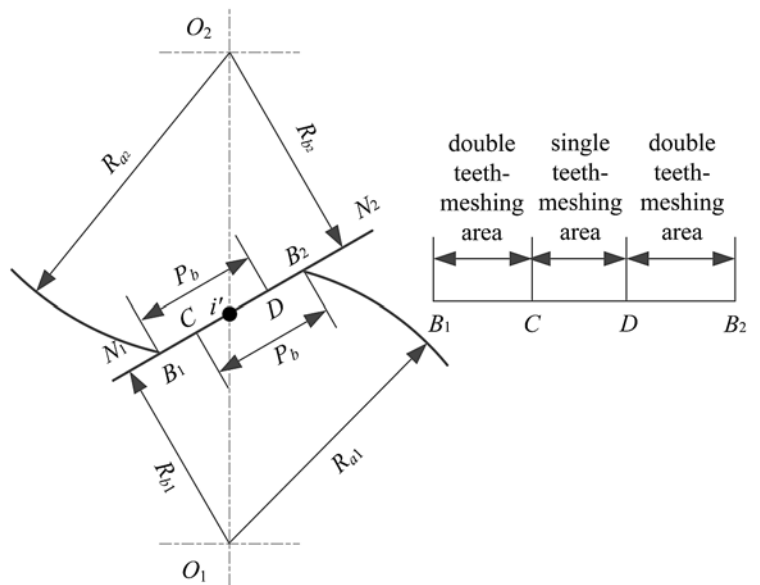

Fig. 1. Schematic diagram of a meshing gear

Take the contact ratio $1<\varepsilon<2$, for instance, as shown in Figure 1. The total transmission load equals the sum of load carried by two adjacent teeth pairs, that is:

$$W = W_1 + W_2 \qquad (1)$$

Where W is total normal load per unit width, W_1 is normal load shared by the first gear pair, W_2 is normal load shared by the second gear pair.

As shown in Figure 2, In case of $e_{t1}<e_{t2}$, the first gear pair contacts firstly, e_{t1} and e_{t2} are composite error of gear pair 1 and 2, where the direction along gear surface dent is positive. δ_1 and δ_2 are elastic deformation of the two gear pairs. $k_1(t)$ and $k_2(t)$ are meshing stiffness per unit width.

According to the principle that the load is proportional to the deformation, W_1 and W_2 can be established as:

$$W_1 = k_1(t) \times (x - e_{t1}) \qquad (2)$$

$$W_2 = k_2(t) \times (x - e_{t2}) \qquad (3)$$

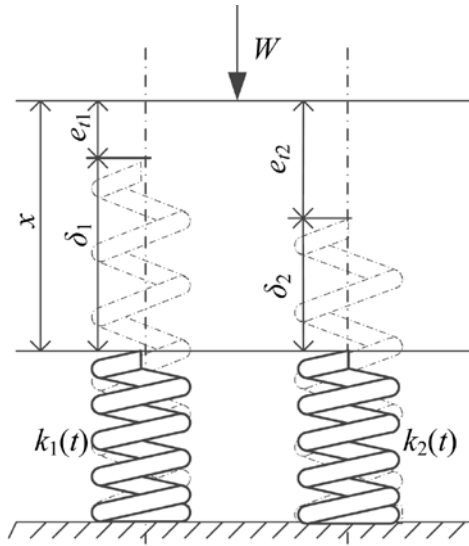Load distribution coefficient β can be obtained by equations (1) to (3), that is:

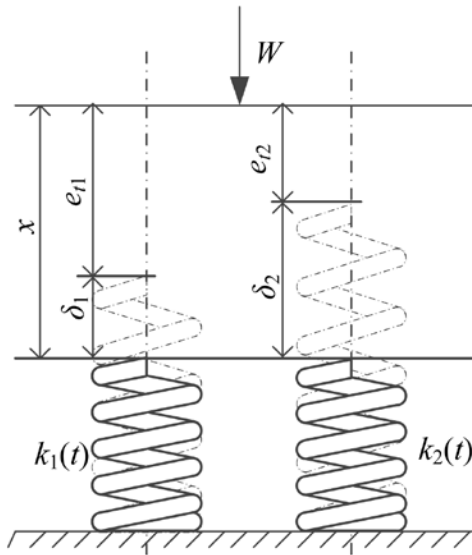Fig. 2. Force diagram of meshing gears (condition 1)

Fig. 3. Force diagram of meshing gears (condition 2)

$$\beta = \frac{W_1}{W} = \frac{k_1(t)}{k_1(t) + k_2(t)} + \frac{k_1(t)k_2(t)}{k_1(t) + k_2(t)} \frac{|\Delta|}{W} \qquad (4)$$

Where $\Delta = e_{t1} - e_{t2}$ is geometric clearance while meshing. Because of $\Delta < 0$, the clearance is occurred in the second gear pair.

The distribution load between the two gear pairs are deduced respectively as:

$$\begin{cases} W_1 = \dfrac{k_1(t)(W + |\Delta| \cdot k_2(t))}{k_1(t) + k_2(t)} \\ W_2 = \dfrac{k_2(t)(W - |\Delta| \cdot k_1(t))}{k_1(t) + k_2(t)} \end{cases} \qquad (5)$$

As shown in Figure 3, the second gear pair mesh firstly, the clearance is occurred in the first gear pair because Δ is more than 0. Load distribution coefficient β is:

$$\beta = \frac{W_1}{W} = \frac{k_1(t)}{k_1(t) + k_2(t)} - \frac{k_1(t)k_2(t)}{k_1(t) + k_2(t)} \frac{|\Delta|}{W} \qquad (6)$$

The distribution load between the two gear pairs are deduced respectively as:

$$\begin{cases} W_1 = \dfrac{k_1(t)(W - |\Delta| \cdot k_2(t))}{k_1(t) + k_2(t)} \\ W_2 = \dfrac{k_2(t)(W + |\Delta| \cdot k_1(t))}{k_1(t) + k_2(t)} \end{cases} \qquad (7)$$

Considering the clearance caused by gear wear, mathematical expression of clearance Δ can be deduced as follows:

When the meshing point is at section B_1C, clearance Δ is:

$$|\Delta| = |h_1(y) + h_2(y) - (h_1(y + p_b) + h_2(y + p_b))| \qquad (8)$$

When the meshing point is at section DB_2, clearance Δ is:

$$|\Delta| = |h_1(y) + h_2(y) - (h_1(y - p_b) + h_2(y - p_b))| \qquad (9)$$

Where y is the distance between contact point i and pitch point i' along the direction of meshing line. $h(y)$ is wear depth per unit width.

3. A numerical prediction model of wear in spur gear

Under high contact pressure, relative rolling and sliding motion occurs at the surfaces of meshing teeth. Most gear sets have oil and grease lubrication; however, lubrication condition is boundary or mixed lubrication. It indicates that meshing surface can't be fully separated by lubricant and occurs directly metal rubbing. Thus, material transfer and peeling metal will be generated at teeth surface under the low speed and heavy-duty condition, which is called as gear wear.

A generalized wear equation, which is called Archard model, is usually used to predict gear wear:

$$\frac{V}{s} = K \frac{W}{H} \qquad (10)$$

Where V is wear volume loss of material, s is sliding distance of meshing gear teeth, W is the applied normal load, H is material hardness of observed surface. K is dimensionless wear coefficient, which is related to lubrication condition and wear mechanism.

Flodin [9] proposed a mild wear model in spur gear. Supposing k is constant, and surface pressure p_i and sliding velocity v_i remain unchanged in a very short time, the wear depth can be expressed as:

$$h_{i,n} = h_{i,n-1} + \Delta t k N \sum_{j=1}^{s} p_{i,j} v_{i,j} \qquad (11)$$

Where $h_{i,n-1}$ is wear depth of mesh point i after n-1 wear cycles, n is present wear cycles, Δt is time increment, N is running revolutions at every interval, during which the profile of gear teeth will not be updated. j is the point within Hertzian contact radius, $p_{i,j}$ is surface pressure of point j, $v_{i,j}$ is sliding velocity of point j.

Surface pressures of contact point i and j within contact radius can be calculated by the Winkler model [12, 17].

$$p_{i,j}(x_{i,j}) = \frac{(0.59 E^*)}{Ra}(a^2 - x_{i,j}^2) \qquad (12)$$

Where, j is the meshing point, a is contact radius, $x_{i,j}$ is distance from point i in contact radius to meshing point j, E^* is equivalent elastic modulus, R is equivalent radius of two rotating cylinders. The computation expressions of indirect variable in equation (12) are:

$$\frac{1}{E^*} = \frac{1 - \mu_1^2}{E_1} + \frac{1 - \mu_2^2}{E_2} \qquad (13)$$

$$\frac{1}{R} = \frac{1}{R_1} + \frac{1}{R_2} \qquad (14)$$

$$R_1 = ia_1 = R_{b_1} \tan \beta_{1i} \qquad (15)$$

$$R_2 = ia_2 = R_{b_2} \tan \beta_{2i} \qquad (16)$$

$$a = \left(\frac{4WR}{\pi E^*} \right)^{1/2} \qquad (17)$$

Where W represents W_1 or W_2, W_1 is shared load by the first teeth pair, W_2 is shared load by the second teeth pair, which can be obtained by equations (5) and (7), E_1, E_2, μ_1, μ_2 are respectively elastic modulus

Fig. 4. The calculation flow chart

and poisson ratio of pinion and gear, R_{b1}, R_{b2} are radiuses of base circle, β_{1i}, β_{2i} are pressure angle of the mesh point i, Φ is engagement angle.

The sliding velocity v_i of meshing point i can be determined by gear mesh theory:

$$v_i = (\omega_1 + \omega_2) \times y_i \qquad (18)$$

$$y_i = ii' = R_{b1}(\tan \beta_{1i} - \tan \phi) = R_{b2}(\tan \phi - \tan \beta_{2i}) \qquad (19)$$

The flow chart for wear calculation is provide in Figure 4.

4. Surrogate models for nonlinear response

4.1. Artificial neural network

Because of the capabilities in pattern classification and function approximation, artificial neural network models are being one of most mature and widely used network models. A simple three-layer BP network can approach any complicated nonlinear function relations. A random vector $\mathbf{X}^T = \{x_1, x_2, ..., x_n, t\}^T$ which consists of original stochastic variables $\{x_1, x_2, ..., x_n\}^T$ and time t is treated as the input parameter of network, and wear depth response $h_i(x_1, x_2, ..., x_n, t)$ is treated as the output parameter of network. The expression of nonlinear function is obtained after training:

$$h_i = f\left(\theta_k + \sum_{j=1}^{m} w_{kj} \delta\left(\theta_j + \sum_{i=1}^{n+1} w_{ji} x_i \right) \right) \qquad (20)$$

where δ is S-type logarithmic function, f is linear function.

$$\delta(x) = \frac{1}{1 + e^{-\beta x}}, \beta > 0 \qquad (21)$$

$$f(x) = x \qquad (22)$$

4.2. Kriging model

On the basis of the kriging method, the stochastic response model is denoted as two parts. The first part is the parametric regression model $F(\beta), x$. The second part is the non-parametric stochastic process model $z(x)$. The response is defined as:

$$h(x) = F(\beta, x) + z(x) = f(x)^T \beta + z(x) \qquad (23)$$

Where x is random variable and h is stochastic response, both of them are assumed to satisfy the normalization conditions. β is regression parameter. $f(x)$ is polynomial equation of x. $z(x)$ is random process and assumed to have mean zero and covariance is:

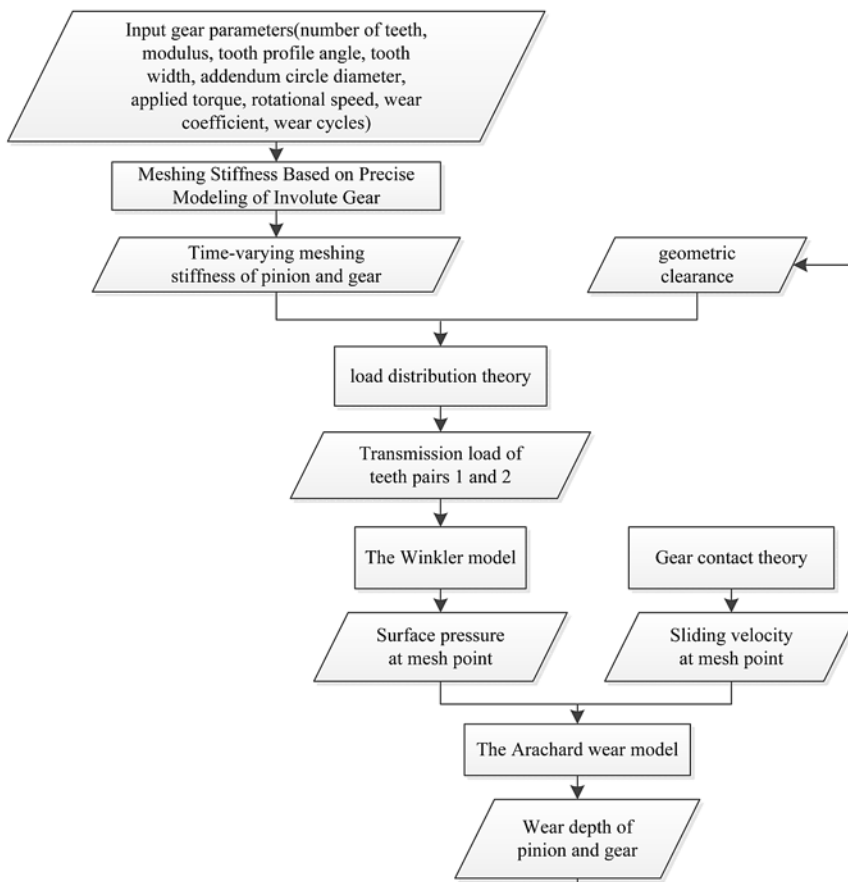$$\text{cov}\left[z(x_i), z(x_j) \right] = \sigma^2 R(\theta_k, x_i, x_j) \qquad (24)$$

Where R is correlation function with 7 common forms, θ_k is the key parameter of the function.

To keep the predictor unbiased, The Kriging approximations are defined as:

$$\hat{h}(x) = f(x)^T \beta^* + r(x)^T R^{-1}(H - F\beta^*) \qquad (25)$$

Where $x=\{x_1, x_2, ..., x_{n+1}\}$ is a vector composed by untried point, n+1 is the number of random variables. $f(x)^T = \{f_1(x), f_2(x), ..., f_p(x)\}$ are polynomials of vector x, p is polynomial order. $\beta^* = \{\beta_1^*, \beta_2^*, ..., \beta_p^*\}^T$ is the generalized least squares solution. Given a set of m design points $x_{s_1}, x_{s_2}, ..., x_{s_m}$, $r(x) = \{R(\theta_k, x, x_{s_1}), R(\theta_k, x, x_{s_2}), ..., R(\theta_k, x, x_{s_m})\}^T$ is the vector of correlation between untried points and design points. $R_{m \times m}$ is correlation matrix between design points. H is response vector of design points. F is design matrix of design points.

β^* is deduced according to the equation below:

$$\beta^* = F^T R^{-1} F^{-1} F^T R^{-1} H \qquad (26)$$

Where $R(\theta_k, x_i, x_j)$ is spatial correlation function of any two design points ($i, j \in s_1, ..., s_m$). And the generalized correlation function is Gaussian function.

$$R(\theta_k, x_i, x_j) = \prod_{k=1}^{n+1} \exp(-\theta_k |x_k^i - x_k^j|^2) \qquad (27)$$

$R(\theta_k, x_i, x_j)$ is assumed to be assembled into the correlation matrix R:

$$R = \begin{bmatrix} \sigma_1^2 & R(x_1, x_2) & ... & R(x_1, x_m) \\ R(x_2, x_1) & \sigma_2^2 & & \\ ... & & & \\ R(x_m, x_1) & & & \sigma_m^2 \end{bmatrix}_{(m \times m)} \qquad (28)$$

The optimal coefficients θ^* of the correlation function is derived by maximum likelihood estimation method:

$$\theta^* = \min_\theta \left\{ |R|^{\frac{1}{m}} \sigma^2 \right\} \qquad (29)$$

Where $|R|$ is the determinant of R.

If the form of correlation function, the order of polynomial and design samples are given, β^* can be calculated by equation (26). And $\hat{h}(x)$ can be obtained by equation (25) when untried points x are given.

5. Reliability analysis method based on the Edgeworth series and four moment techniques

Gear wear accumulates gradually along with time. System failure is said to have occurred due to wear over the threshold value. As the wear speed and threshold of driving wheel are different from driven wheel, the reliability model of the driving and driven wheel need to be built respectively. Taking driving wheel as an example, according to the safety criterion that maximum wear depth on the tooth profile are not allowed to exceed specified clearance, the limited state function of driving wheel is defined as:

$$g_p(x,t) = E_{sni}^p - \max(h_i^p(x,t)) \qquad (30)$$

Where $h_i(x,t)$ is wear depth of meshing point i at any time t, E_{sni} is lower deviation of tooth thickness and maximum clearance allowed.

The failure probability of driving wheel is formulated as follows:

$$P_{fc}^p = P\left[g_p(x,t) \leq 0 \right] = F_{g_p}(0) \qquad (31)$$

The reliability of driving wheel can be expressed by equation (32):

$$R_p(t) = P\left[g_p(x,t) > 0 \right] = 1 - P_{fc}^p = \int_{g(x)>0} f(x) dx \qquad (32)$$

According to equation (32), the expression of limited state function and probability distribution of original variables are necessary precondition to calculate reliability. However, both of them can't be obtained due to lack of the statistical data and complex structure. To solve the problem, the arbitrary distribution function of the standard random variable is approximately expressed by the standard normal distribution function using the Edgeworth series[25] as follows:

$$F(y) = \Phi(y) - \varphi(y)\left[\frac{1}{6}\frac{\theta_g}{\sigma_g^3}H_2(y) + \frac{1}{24}\left(\frac{\eta_g}{\sigma_g^4} - 3\right)H_3(y) + \frac{1}{72}\left(\frac{\theta_g}{\sigma_g^3}\right)^2 H_5(y) + ... \right] \qquad (33)$$

where $\phi(\cdot)$ is the standard normal probability density function, and $H_i(y)$ is the Hermite polynomial, $\sigma_g \theta_g \eta_g$ are the variance, the third moment, and the fourth moment of the limited state function, which can be expressed by the corresponding moments of the random variables as follows based on the four moment method:

$$\mu_g = E[g_d(X) + \varepsilon g_p(X)] = g_d(X) \qquad (34)$$

$$\sigma_g^2 = Var[g(X)] = \left(\frac{\partial g_d(X)}{\partial X^T}\right)^{[2]} Var(X) \qquad (35)$$

$$\theta_g = E[g(X) - g_d(X)]^3 = \left(\frac{\partial g_d(X)}{\partial X^T}\right)^{[3]} C_3(X) \qquad (36)$$

$$\eta_g = E[g(X) - g_d(X)]^4 = \left(\frac{\partial g_d(X)}{\partial X^T}\right)^{[4]} C_4(X) \qquad (37)$$

Where Var(X) is the variance matrix that includes all variances and covariances of the random parameters. $C_3(X)$, $C_4(X)$ are the third and fourth moment matrices comprised by all the third and fourth central moments of each random parameter. Var(X), $C_3(X)$, $C_4(X)$ can be figured out by parameter estimation method. The Kronecker power is $(\cdot)^{[k]} = (\cdot)^{[k-1]} \otimes (\cdot) = (\cdot) \otimes (\cdot) \otimes \cdots \otimes (\cdot)$, and the symbol $\otimes$ represents the Kronecker product which is defined as $(A)_{p \times q} \otimes (B)_{s \times t} = [a_{ij}B]_{ps \times qt}$. $\partial g_d / \partial x_i$ can be calculated by taking a derivative with respect to ANN surrogate model.

Thus, the reliability R is represented as:

$$R_p(t) = 1 - P_{fc}^p = 1 - F(-\beta) \qquad (38)$$

Where $\beta = \dfrac{\mu_g}{\sigma_g}$ is reliability index.

Substituting β into equation (33), the reliability of driving wheel is derived from equation (38).

6. Examples

Supposing the level of gear precision is 6, gear parameters are listed out in Table 1. The former is assumed to be deterministic, the latter are random and the four moments are given.

Table 1. Parameters of gear pair

Parameter	Code and size	Parameter	Code and size
Teeth number-driving	$z_1 = 24$	Modulus	$m_n = 4.5$mm
Teeth number-driven	$z_2 = 26$	Pitch diameter-driving	$d_{w1} = 108$mm
Center distance	$a_w = 112.5$mm	Pitch diameter-driven	$d_{w2} = 117$mm

Parameter	Mean value	The four moments
Nominal pressure angle	$\alpha_n = 20°$	(20, 1, -0.00177972, 2.99779)
Tooth width	$b = 15$mm	(15, 0.2025, 0.0081733, 0.123569)
Applied torque	$T_1 = 302000$N·mm	(3.02e5, 9.1204e6, -1.35432e7, 2.4919e14)
Driving gear speed	$n_1 = 150$r/min	(150, 100, 199.505, 30749.6)
Wear coefficient	$k = 5 \times 10^{-10}$mm²N⁻¹	(5e-10, 3.6e-21, -6.28011e-35, 3.88836e-41)

6.1. Numerical solution of wear depth in gears

The time varying meshing stiffness can be calculated by the precise modeling of involute gear[23,24], as shown in Figure 5, the stiffness curve of a pair of teeth is given.
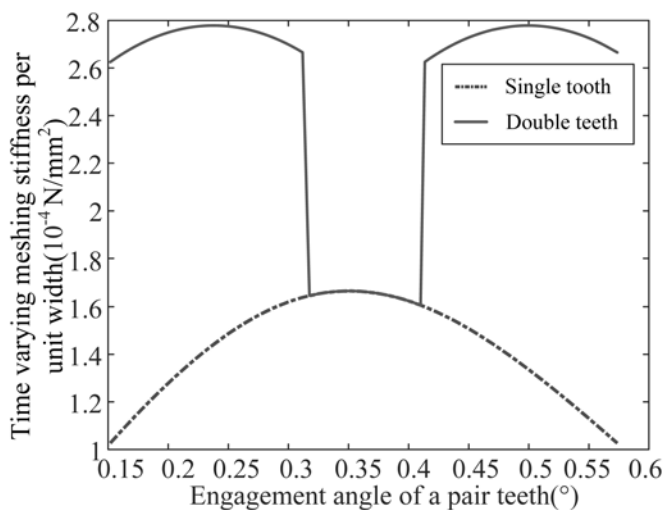

Fig. 5. Time varying meshing stiffness curves of single and double teeth based on precise modeling of involute gear
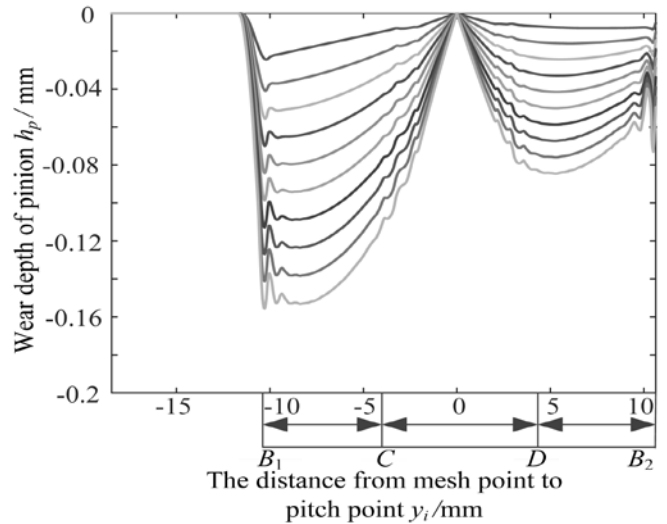

Fig. 6. Wear depth of the pinion after n wear cycles

Supposing the total wear cycle is 300, the gear wheel rotates 5000 circles (that is N=5000) after one wear cycle. In any circle, tooth profile, surface pressure and sliding velocity remain to be constant.

The wear of the pinion and gear after n wear cycles are presented in the figure (6) and (7). To facilitate making clear drawing, the results of wear depth after 30, 60, ……,300 cycles are plotted in figures by the distance from meshing point to pitch point on the horizontal axis. According to the principle of gear engagement shown in Figure 1, the B1 point is start of engagement and B2 is end of engagement. The zero value is at pitch point, the negative is at points from base circle to pitch point, and the positive is from pitch point to addendum circle. The wear depths of the pinion and gear respectively are varying over the teeth flanks with the maximum wear at the root and minimum wear at the pitch. The wear of driving pinion is more than driven gear, which agrees with the conclusion in references[1,21].
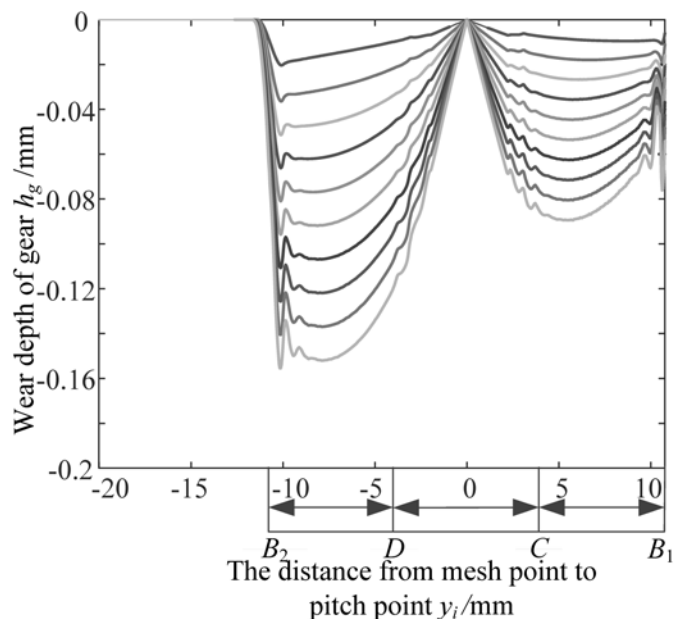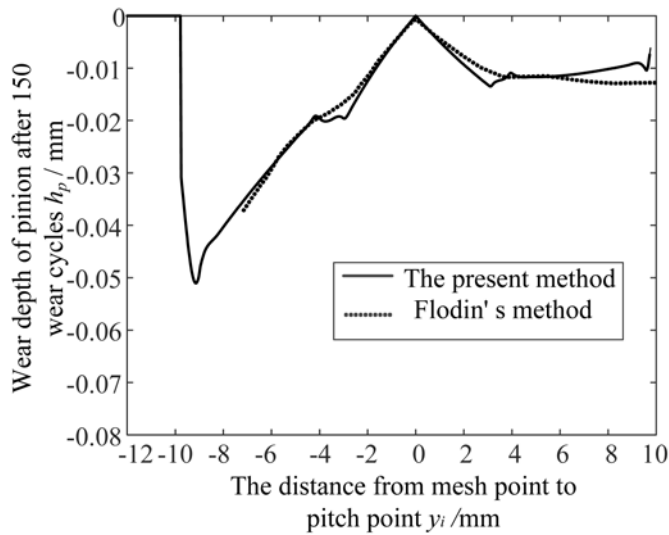

Fig. 7. Wear depth of the gear after n wear cycles

Fig. 8. *Comparison of wear depth with the present method and Flodin's method*

Fig. 10. *Comparison of gradual wear process in driven wheel under different sample sizes with ANN method*

As the time-varying stiffness and the distribution load are both considered in present paper, wear depths at the conversion position of single teeth-meshing area and double teeth-meshing area are fluctuating slightly and don't appear sudden change while this phenomenon has appeared in reference[2] where the load is distributed equally. The wears are varying from pitch to addendum but drastically from root to pitch.

Based on the gear parameters in reference [9], wear depth with the method in the present paper are compared with Foldin's. Considering distributed load between two gear pairs, wear depths of the pinion with the two methods are shown in figure 8, and the results are very close.

6.2. ANN and Kriging surrogate models

A random vector $X^{\mathrm{T}} = \{x_1, x_2, ..., x_n, t\}^{\mathrm{T}}$ which consists of original stochastic variables $\{x_1, x_2, ..., x_n\}^{\mathrm{T}}$ and time t is treated as the input parameter of network, and wear depth response $h_i(x_1, x_2, ..., x_n, t)$ is treated as the output parameter of network. Three-layer BP neutral network models with a 6-13-1 form are structured when sample sizes are 50,100 and 500 respectively (see Appendix A). Log-sigmoid function is selected as the transfer function of hidden layer. Purelin function is selected as the transfer function of output layer. Trainlm func-

Fig. 11. *Comparison of gradual wear process in driving wheel under different sample sizes with Kriging method*
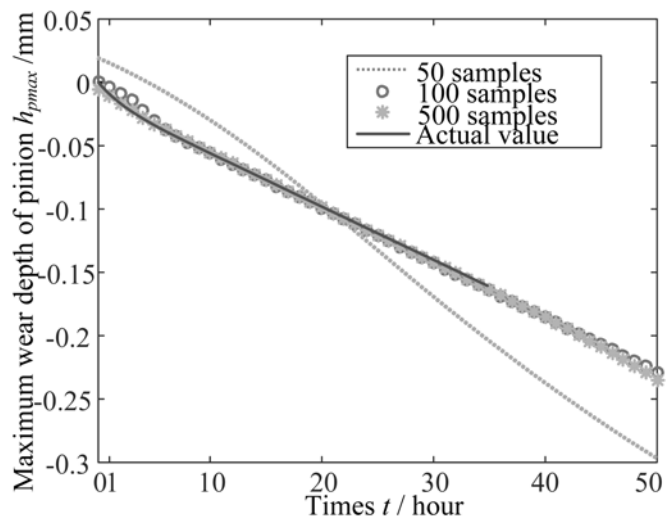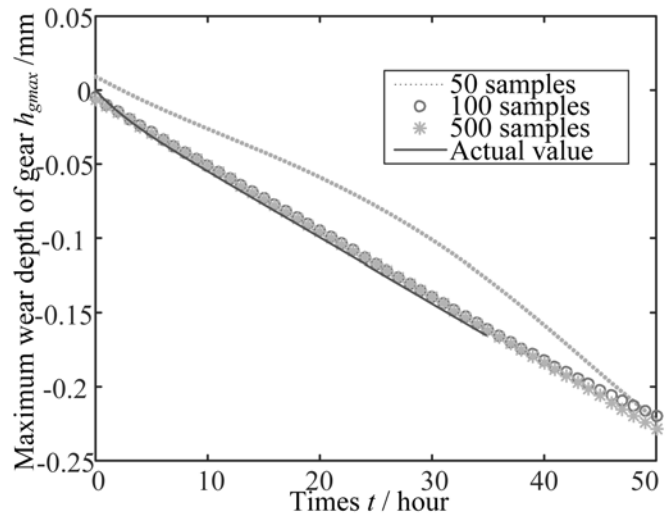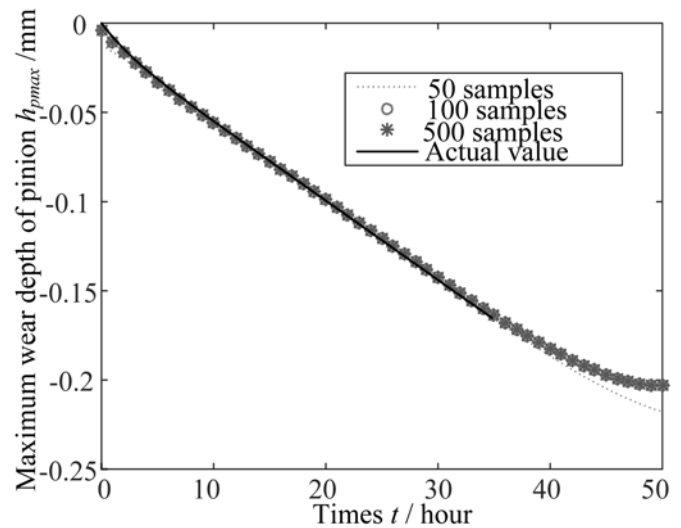

Fig. 9. *Comparison of gradual wear process in driving wheel under different sample sizes with ANN method*
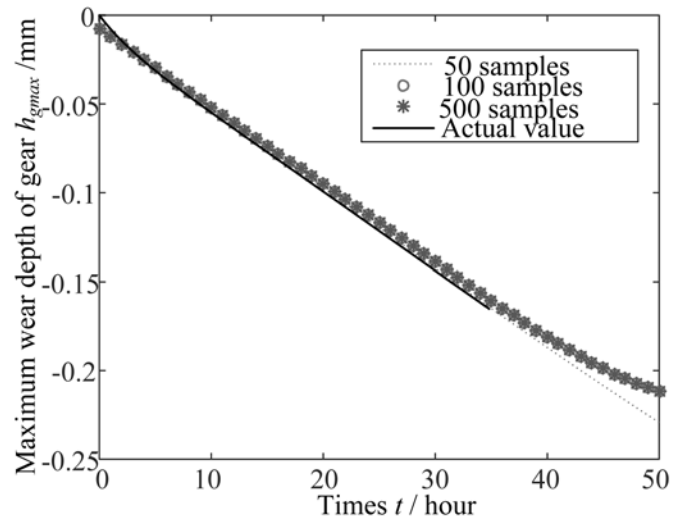

Fig. 12. *Comparison of gradual wear process in driven wheel under different sample sizes with Kriging method*

tion is selected as training function. The training terminates if network error is less than 10^{-6}. The training parameters of ANN are listed out in Appendix B.

To determine the suitable sample size, both of the accuracy and goodness of fit needed to be tested for the three network models with different samples. The accuracy means comparison of gradual wear process between exact and surrogate models when original stochastic variables $\{x_1, x_2, ..., x_n\}^T$ are deterministic and equal to the mean values. The goodness of fit means comparison of wear depths between
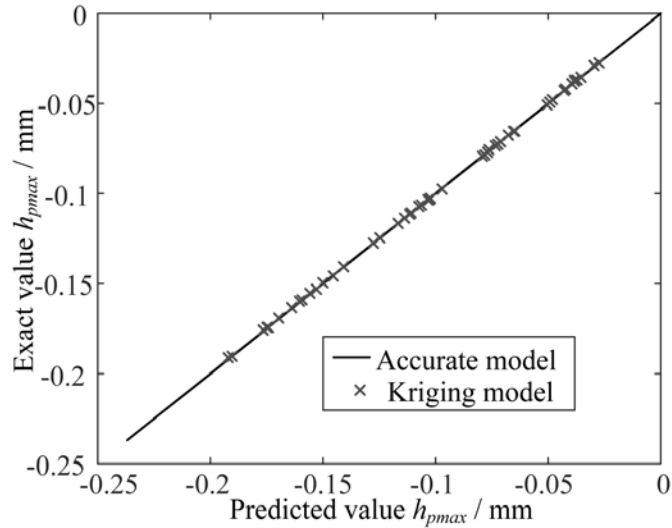

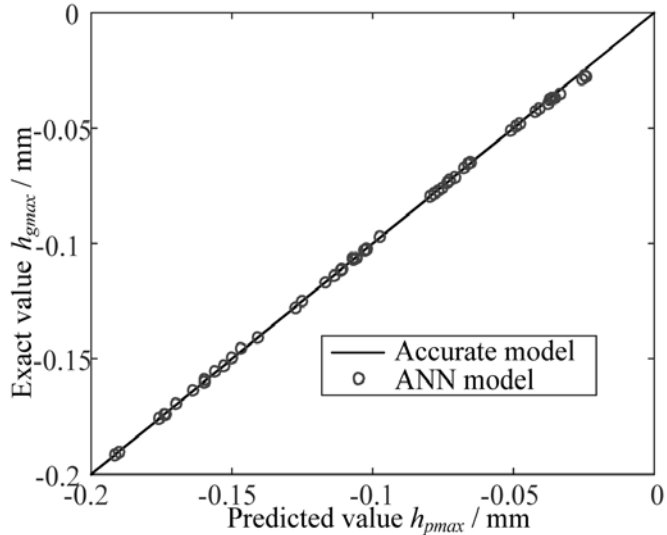Fig. 13. Approximate values with Kriging method and Actual values of driving wheel

Fig. 14. Approximate values with Kriging method and Actual values of driven wheel

the two models with another set of samples when time is deterministic.

The accuracy of driving and driven wheels with ANN model are figured as follows:

As shown in figures 9 and 10, the accuracy is low with 50 samples whereas high with 100 and 500 samples. And the latter two make accurate prediction on the developing trend of wear depth.

The accuracy of driving and driven wheels with Kriging model are figured as follows:

As shown in figures 11 and 12, all of three models have high accuracy and make accurate prediction on the developing trend. It shows that Kriging method needs less samples than ANN method under the same accuracy.

Figures 13 and 14 shows goodness of fit based on ANN and Kriging surrogate models with 100 samples. Results of the other two are shown in Table 2.

The goodness of fit for ANN models with 100 and 500 samples can reach more than 0.9999. But the 50-samples model has a low goodness of fit so that can't be used. The goodness of fit for Kriging models with all samples can reach more than 0.96. In a comprehensive view, the suitable sample size for ANN model is more than 100, for Kriging more than 50.

6.3. Reliability curve

The permitted maximum clearances of driving and driven wheels are -142μm and -143μm respectively. On the basis of ANN surrogate models, combining with Edgeworth series and four moment method, the time-dependent reliability curve can be obtained under the condition that the four moments of original variables are known but the probability distribution unknown. Reliability curve can be also obtained with Kriging-based MCS method. Supposing probability distribution are known is convenient to make comparison of the ANN-Edgeworth Series-Four moment method and Kriging-MCS method,
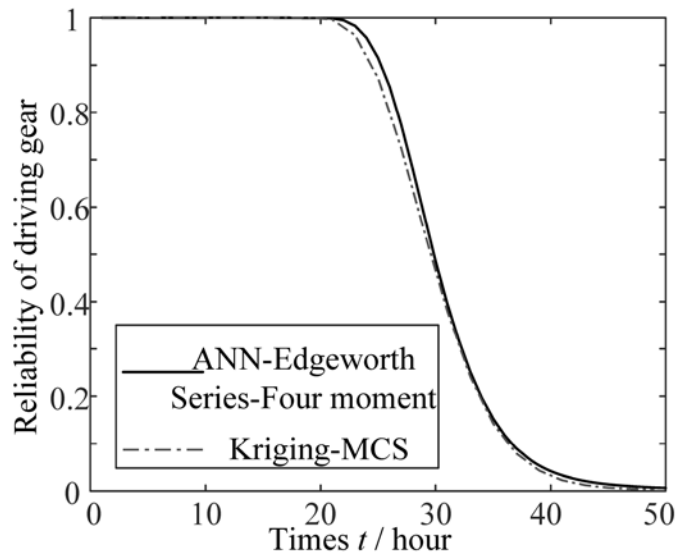
Fig. 15. Reliability curves of driving wheel

which are shown in Figures 15 and 16.

Reliability remains to be 1 in the beginning for a long time. After 20 hours, reliability decreases gradually and becomes 0 at 50 hours. It is important to note that the applied load in the present paper is much larger than that in practice to save time. And product life under normal load are longer than test load. However, the

Table 2. Goodness of fit for ANN and Kriging models with different sample sizes

Sample size	ANN		Kriging	
	Driving wheel	Driven wheel	Driving wheel	Driven wheel
50	0.74318433	0.60040412	0.98699443	0.96489048
100	0.99990496	0.99997755	0.99997951	0.97556336
500	0.99997285	0.99997416	0.99997951	0.97556336
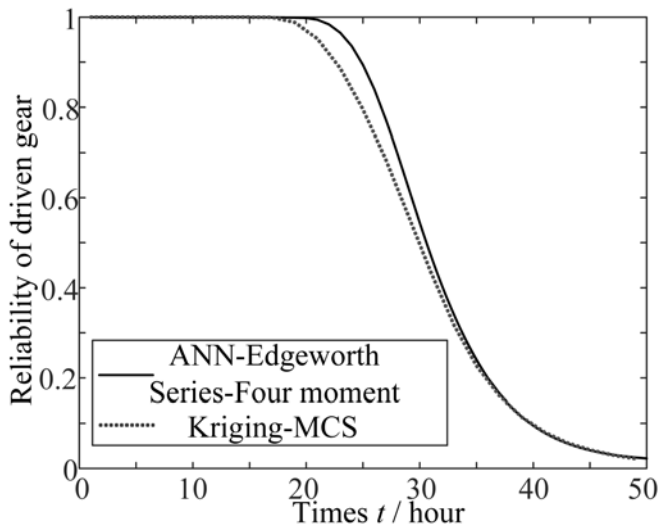
Fig.16. Reliability curves of driven wheel

3.8 years, which is impossible to complete. The former two only need tens of hours, which has a high efficiency.

7.conclusions

The present paper studied dynamic evolution law of mechanical reliability caused by wear. A numerical wear model has been established considering dynamic distribution load of gear tooth. Wear depths and gradual law has been obtained. Wear random process has been introduced. The problem of time-dependent reliability analysis with complex structural has been solved. The main conclusions are:

(1) Load and wear are coupled with each other. The dynamic characteristic of gear system is affected by variation of geometrical shape and dimension parameter caused by mild wear and dynamic load will lead to more serious wear. Thus, time-varying stiffness and dynamic distribution load should be both considered into wear model. As a result, sudden change hasn't appeared at the conversion point of single and double meshing area.

(2) Wear calculation spends a lot of time so that direct MCS method is not suitable for reliability analysis. It necessary to develop a surrogate model to replace exact model. Both of ANN and Kriging models have a high accuracy and goodness of fit. Kriging model needs less samples than ANN.

(3) Under the condition that the probability functions of random variables are unknown, Edgeworth series and four moment methods can be used to calculate reliability.

(4) Both of ANN-Edgeworth series-Four moment method and Kriging-MCS method are suitable for reliability with complex structure and have little difference.

Table 3. Consuming time of the three methods

Method	Sample size	Original samples	Program	Total
ANN-Edgeworth -Four moment	100	33.3 hours	10 seconds	34 hours
Kriging-MCS	50	16.7 hours	2 minutes	17 hours
Direct-MCS	10^5	3.8 years	10 seconds	3.8 years

present paper is focus on studying gradually law of wear reliability and choosing the suitable method to solve complex problem. According to the results with two methods, ANN-Edgeworth Series-Four moment method is a little bigger than Kriging-MCS method. That is to say, the difference is only a little. Supposing the time which is spent running the exact wear model once is 20 minutes, consuming time of every method for reliability is listed in Table 3.

The time for building up original samples account for absolute proportion, about more than 99% of the total. If more original samples the method needs, more time it will consume. As the direct-MCS method needs a large number of samples, the cost of time is as high as

Appendix A

Table 1. Original samples for construct ANN and Kriging models (50samples)

α_n	b	k	n_1	T_1	t	hgmax	hpmax
21.152	14.577	5.64E-10	144.85	294587.3	24853.3	-0.03447	-0.04364
21.152	14.577	5.64E-10	144.85	294587.3	49706.59	-0.06479	-0.07621
21.152	14.577	5.64E-10	144.85	294587.3	74559.89	-0.09522	-0.1085
21.152	14.577	5.64E-10	144.85	294587.3	99413.19	-0.12574	-0.14088
21.152	14.577	5.64E-10	144.85	294587.3	124266.5	-0.15607	-0.17364
19.778	14.986	4.69E-10	164.85	296417.6	21838.03	-0.03494	-0.03853
19.778	14.986	4.69E-10	164.85	296417.6	43676.07	-0.06283	-0.06556
19.778	14.986	4.69E-10	164.85	296417.6	65514.1	-0.09021	-0.09225
19.778	14.986	4.69E-10	164.85	296417.6	87352.14	-0.11774	-0.11871
19.778	14.986	4.69E-10	164.85	296417.6	109190.2	-0.14519	-0.14518
20.667	15.641	3.64E-10	155.15	298247.9	23203.35	-0.02374	-0.03
20.667	15.641	3.64E-10	155.15	298247.9	46406.7	-0.0434	-0.05069
20.667	15.641	3.64E-10	155.15	298247.9	69610.05	-0.06262	-0.07035
20.667	15.641	3.64E-10	155.15	298247.9	92813.41	-0.08188	-0.09002
20.667	15.641	3.64E-10	155.15	298247.9	116016.8	-0.10123	-0.10964
20.545	16.186	3.38E-10	124.85	300078.2	28834.6	-0.02206	-0.02766
20.545	16.186	3.38E-10	124.85	300078.2	57669.2	-0.04014	-0.04659
20.545	16.186	3.38E-10	124.85	300078.2	86503.8	-0.05755	-0.06439
20.545	16.186	3.38E-10	124.85	300078.2	115338.4	-0.07489	-0.08219
20.545	16.186	3.38E-10	124.85	300078.2	144173	-0.09221	-0.09982
19.899	13.977	3.89E-10	173.94	301908.5	20696.79	-0.03208	-0.03652
19.899	13.977	3.89E-10	173.94	301908.5	41393.58	-0.05761	-0.06161
19.899	13.977	3.89E-10	173.94	301908.5	62090.38	-0.08244	-0.0859
19.899	13.977	3.89E-10	173.94	301908.5	82787.17	-0.1073	-0.11022
19.899	13.977	3.89E-10	173.94	301908.5	103484	-0.1322	-0.13466
18.121	15.886	4.62E-10	162.42	303738.8	22164.76	-0.04406	-0.03855
18.121	15.886	4.62E-10	162.42	303738.8	44329.52	-0.07505	-0.06409
18.121	15.886	4.62E-10	162.42	303738.8	66494.27	-0.10521	-0.09326
18.121	15.886	4.62E-10	162.42	303738.8	88659.03	-0.13548	-0.12331
18.121	15.886	4.62E-10	162.42	303738.8	110823.8	-0.16565	-0.15342
18.323	14.55	4.15E-10	138.18	305569.1	26052.97	-0.04292	-0.03892
18.323	14.55	4.15E-10	138.18	305569.1	52105.95	-0.07331	-0.06432
18.323	14.55	4.15E-10	138.18	305569.1	78158.92	-0.10252	-0.09107
18.323	14.55	4.15E-10	138.18	305569.1	104211.9	-0.13183	-0.12003
18.323	14.55	4.15E-10	138.18	305569.1	130264.9	-0.16107	-0.14937
18.727	13.923	5.93E-10	152.12	307399.4	23665.53	-0.05548	-0.0523
18.727	13.923	5.93E-10	152.12	307399.4	47331.05	-0.0983	-0.09039
18.727	13.923	5.93E-10	152.12	307399.4	70996.58	-0.14104	-0.13121
18.727	13.923	5.93E-10	152.12	307399.4	94662.11	-0.18369	-0.17359
18.727	13.923	5.93E-10	152.12	307399.4	118327.6	-0.22698	-0.21605
20.263	14.277	3.42E-10	154.55	309229.7	23293.43	-0.02717	-0.03282
20.263	14.277	3.42E-10	154.55	309229.7	46586.87	-0.04913	-0.05515
20.263	14.277	3.42E-10	154.55	309229.7	69880.3	-0.07032	-0.07624
20.263	14.277	3.42E-10	154.55	309229.7	93173.73	-0.09143	-0.09723
20.263	14.277	3.42E-10	154.55	309229.7	116467.2	-0.11253	-0.11821
19.333	14.032	4.55E-10	143.64	311060	25062.66	-0.04084	-0.04273
19.333	14.032	4.55E-10	143.64	311060	50125.31	-0.07248	-0.07243
19.333	14.032	4.55E-10	143.64	311060	75187.97	-0.10338	-0.10184
19.333	14.032	4.55E-10	143.64	311060	100250.6	-0.13439	-0.13116
19.333	14.032	4.55E-10	143.64	311060	125313.3	-0.16523	-0.16045

Appendix B

Table 2. ANN network parameters of driving wheel

[w_{ij}]						[w_{kj}]$^{\mathrm{T}}$	[θ_j]	[θ_k]
-5.22528	3.221899	24.04881	6.898731	2.740079	4.032272	-0.03077	-25.2424	
-0.06841	-0.65284	-1.66892	-3.01045	0.020653	-32.8203	0.108727	-26.8177	
-0.1639	1.876093	-0.32824	-0.93095	-0.80379	-0.14147	0.075344	-1.37843	
1.542938	-0.11529	-0.79372	-0.09672	0.060053	-3.12393	-0.09169	-0.76465	
0.06194	0.044609	-0.43121	-0.40289	-0.01041	-0.42879	4.683095	0.681912	
-0.28528	0.255703	1.007548	-0.78453	-0.03665	1.71228	-0.16621	-0.0539	
-0.05235	-0.10145	0.622529	0.442877	0.038716	-0.28308	2.116904	-0.67204	-50.9805
0.030045	0.100637	0.503045	-0.64295	0.015263	-0.97372	-1.26834	2.260346	
20.95529	-36.4756	-22.8803	3.913039	1.30388	5.377841	-0.00581	-16.6671	
0.193283	0.254279	-0.56163	-0.51449	-0.06677	-0.10976	73.87332	2.798588	
3.921268	-0.26835	-0.90545	-0.38699	0.114956	-1.64071	-25.2716	2.025285	
-0.18652	-0.23793	0.555175	0.509348	0.062009	0.032582	83.42451	-2.94615	
-3.9177	0.269415	0.902563	0.385194	-0.115	1.63199	-25.2959	-2.02856	

Table 3. ANN network parameters of driving wheel

[w_{ij}]						[w_{kj}]$^{\mathrm{T}}$	[θ_j]	[θ_k]
10.01178	-17.8146	22.13516	1.454345	2.592017	5.142662	-0.01478	-25.1922	
0.11027	0.021028	0.363776	0.255979	-0.12823	-1.28498	-1.07677	2.467814	
-0.43166	-0.2898	0.638186	0.470036	-0.00758	0.002081	-4.09345	-2.03569	
-0.75759	0.216657	-0.46778	-1.69948	-0.11459	-31.0365	0.057017	-23.707	
0.044053	0.010625	-1.01128	0.65242	0.021075	0.0022	18.38031	0.173905	
-12.0028	8.778236	-23.4791	6.552863	13.23493	-4.59593	0.011259	20.71292	
-0.03192	-0.00961	1.015037	-0.65358	-0.01902	-0.02486	18.37038	-0.19951	-38.4905
0.143736	0.068286	-0.34145	-0.1845	-0.08919	-0.69346	4.502442	1.447148	
-3.04415	1.357087	-5.2511	1.515298	0.611239	-0.9471	0.021985	-0.02036	
-3.51331	-0.49121	1.019266	-0.42602	0.977701	1.087055	-0.04405	-2.40367	
-100.164	93.57081	-102.359	-49.2258	81.14516	3.081073	0.006283	-81.5959	
-0.31274	-0.21189	0.559268	0.363906	0.02836	-0.47226	7.562517	-2.52769	
2.749156	0.427162	-1.59628	-0.66692	-0.30248	-2.4033	17.67943	10.17811	

References

1. Amarnath M, Sujatha C, Swarnamani S. Experimental studies on the effects of reduction in gear tooth stiffness and lubricant filmthickness in a spur geared system. Tribology International 2009, 42: 340-352, https://doi.org/10.1016/j.triboint.2008.07.008.
2. Andersson S. Partial EHD theory and initial wear of gears, Stockholm: Royal Institute of Technology, 1975.
3. Archard J F. Contact and rubbing of flat surfaces. Journal of applied physics 1953, 24(8): 981-988, https://doi.org/10.1063/1.1721448.
4. Brandão J A, Martins R, Seabra J H O, Castro M J D. An approach to the simulation of concurrent gear micropitting and mild wear. Wear 2015, 324-325: 64-73, https://doi.org/10.1016/j.wear.2014.12.001.
5. Devooght J, Smidts C. Probabilistic reactor dynamics. I: The theory of continuous event trees. Nuclear science and engineering 1992, 111(3): 229-240, https://doi.org/10.13182/NSE92-A23937.
6. Dhanasekaran S, Gnanamoorthy R. Gear tooth wear in sintered spur gears under dry running conditions. Wear 2008, 265: 81-87, https://doi.org/10.1016/j.wear.2007.08.025.
7. Dugan J B, Bavuso S J, Boyd M A. Dynamic fault-tree models for fault-tolerant computer systems. Reliability, IEEE Transactions on 1992, 41(3): 363-377.
8. Flodin A. Wear of spur and helical gears, Stockholm: Royal Institute of Technology, 2000.
9. Flodin A, Andersson S. Simulation of mild wear in spur gears. Wear 1997, 207(1): 16-23, https://doi.org/10.1016/S0043-1648(96)07467-4.
10. Gomes H M, Awruch A M. Comparison of response surface and neural network with other methods for structural reliability analysis. structural safety 2004, 26(1): 49-67.
11. Hashim M, Yoshikawa H, Matsuoka T, Yang M. Considerations of uncertainties in evaluating dynamic reliability by GO-FLOW methodology - example study of reliability monitor for PWR safety system in the risk-monitor system. Journal of Nuclear Science and Technology 2013, 50(7): 695-708, https://doi.org/10.1080/00223131.2013.790304.

12. Johnson K L. CONTACT MECHANICS, Cambridge University Press, Cambridge, 1985.
13. Li X-T, Tao L-M, Jia M. A Bayesian networks approach for event tree time-dependency analysis on phased-mission system. Eksploatacja i Niezawodnosc – Maintenance and Reliability 2015; 17 (2): 273–281, http://dx.doi.org/10.17531/ein.2015.2.15.
14. Onishchenko V. Tooth wear modeling and prognostication parameters of engagement of spur gear power transmissions. Mechanism and Machine Theory 2008, 43: 1639-1664, https://doi.org/10.1016/j.mechmachtheory.2007.12.005.
15. Põdra P. FE Wear Simulation of Sliding Contacts, Stockholm: Royal Institute of Technology, 1997.
16. Park D, Kahraman A. A surface wear model for hypoid gear pairs. Wear 2009, 267(9): 1595-1604, https://doi.org/10.1016/j.wear.2009.06.017.
17. Po˜dra P, Andersson S r. Wear simulation with the Winkler surface model. Wear 1997, 207: 79-85, https://doi.org/10.1016/S0043-1648(96)07468-6.
18. Tan X H, Bi W H, Hou X L, Wang W. Reliability analysis using radial basis function networks and support vector machines. Computers and Geotechnics 2011, 38(2): 178-186, https://doi.org/10.1016/j.compgeo.2010.11.002.
19. Tombuyses B, Devooght J. Solving Markovian systems of O.D.E. for availability and reliability calculations. Reliability Engineering & System Safety 1995, 48: 47-55, https://doi.org/10.1016/0951-8320(94)00065-V.
20. Volovoi V. Modeling of system reliability Petri nets with aging tokens. Reliability Engineering & System Safety 2004, 84(2): 149-161, https://doi.org/10.1016/j.ress.2003.10.013.
21. Wang S R, Yan Y T, Ding J Y. Experimental Study on Mesh-wear of Involute Spur Gears. Journal of Northeastern University(Natural Science) 2004, 25(2): 146-149.
22. Wang Z, Xie L Y. Time-Dependent Reliability Theory and Method of Mechanical Component, Science Press, Beijing, 2012.
24. Zhang K X, Hu P, Zhang Y M. Numerical Calculation of Meshing Stiffness Based on Precise Modeling of Involute Gear. Machinery Design & Manufacture 2013, (2): 66-73.
25. Zhang Y M, Wen B C, Liu Q L. First passage of uncertain single degree-of-freedom nonlinear oscillators. Computer Methods in Applied Mechanics and Engineering 1998, 165(1-4): 223-231, https://doi.org/10.1016/S0045-7825(98)00042-5.
26. Zhang Y M, Wen B C, Liu Q L. Reliability sensitivity for rotor-stator systems with rubbing. Journal of Sound and Vibration 2003, 259(5): 1095-1107, https://doi.org/10.1006/jsvi.2002.5117.
27. Zhu Z F, Du X P. Reliability Analysis With Monte Carlo Simulation and Dependent Kriging Predictions. Journal of Mechanical Design 2016, 138(12): 121403, https://doi.org/10.1115/1.4034219.
28. Żurowski , Brzózka K, Górka B. Analysis of surface layers and wear products by Mössbauer spectral analysis, Wear 2013, 297: 958-965, https://doi.org/10.1016/j.wear.2012.10.012.

Lisha ZHU
1. School of Mechanical and Automotive Engineering
Zhaoqing University
Zhaoqing Avenue, Duanzhou District, Zhaoqing, Guangdong, 526061, P.R. China
2. School of Mechanical Engineering and Automation
Northeastern University
NO. 3-11, Wenhua Road, Heping District
Shenyang, Liaoning, 110819, P.R. China

Yimin ZHANG
1. School of Mechanical and Automotive Engineering
Zhaoqing University
Zhaoqing Avenue, Duanzhou District, Zhaoqing, Guangdong, 526061, P.R. China
2. Institute of Equipment Reliability
Shenyang University of Chemical Technology
NO. 11 Road, Economic and Technical Development Zone
Shenyang, Liaoning, 110142, P.R. China

Rui ZHANG
School of Mechanical Engineering and Automation
Northeastern University
NO. 3-11, Wenhua Road, Heping District
Shenyang, Liaoning, 110819, P.R. China

Peiming ZHANG
Guangxi Research Institute Mechanical Industry
NO. 5, Chuangxin Road, Xixiang tang District
Nanning, Guangxi, 530000, P.R. China

E-mails: neulisachu@163.com, ymzhang@mail.neu.edu.cn, 15940256305@163.com, 1357889106@qq.com